PHYSICAL REVIEW B **83**, 195427 (2011)

Evolution of the Rashba spin-orbit-split Shockley state on Ag/Pt(111)

Azzedine Bendounan,[1,2,*] Kamel Aït-Mansour,[3,4] Jürgen Braun,[5,†] Jan Minár,[5] Sven Bornemann,[5] Roman Fasel,[3] Oliver Gröning,[3] Fausto Sirotti,[1] and Hubert Ebert[5]

[1]*Synchrotron SOLEIL, L'Orme des Merisiers, Saint-Aubin, BP 48, FR-91192 Gif-sur-Yvette Cedex, France*

[2]*Swiss Light Source, Paul Scherrer Institute, CH-5232 Villigen PSI, Switzerland*

[3]*Empa, nanotech@surfaces Laboratory, Feuerwerkerstrasse 39, CH-3602 Thun, Switzerland*

[4]*Ecole Polytechnique Fédérale de Lausanne, IPMC, Station 3,CH-1015 Lausanne, Switzerland*

[5]*Department Chemie und Biochemie, Physikalische Chemie, Ludwig-Maximilians Universität München, DE-81377 München, Germany*

(Received 18 March 2011; published 17 May 2011)

We have studied the evolution of the Pt(111) Shockley-type surface state, which can be described as a surface resonance upon deposition of Ag monolayers. We have combined angle-resolved photoemission and scanning-tunneling-spectroscopy measurements with electronic-structure and photoemission calculations for true semi-infinite systems to guarantee a complete description of all surface-sensitive spectral features. An unusual energy shift and a considerable Rashba-type spin-orbit splitting of the surface resonance were observed and are discussed in terms of modifications in the electronic structure and relationship between the semi-infinite bulk and the surface potential via multiple electron scattering. The maximum magnitude of the splitting in momentum space amounts to 0.051 ± 0.007 Å^{-1} and appears as one of the highest values so far observed in the $\bar{\Gamma}$-type surface-state-resonance bands.

DOI: 10.1103/PhysRevB.83.195427 PACS number(s): 73.20.At, 71.15.−m, 71.70.Ej, 79.60.−i

I. INTRODUCTION

Angle-resolved photoemission (ARPES) is one of the leading spectroscopic techniques concerning the investigation of surface properties because the method provides, due to its surface sensitivity, a direct access to the surface electronic structure of arbitrary two-dimensional structures. During the last decade a tremendous progress was triggered by qualitative and quantitative improvements. Modern experimental arrangements consisting of new photon sources, analyzers, and detector supplies permit extremely high angle, energy, and, if necessary, spin resolutions.[1] High resolution provides a major advantage in the study of very detailed properties of surface emission and, in particular, the influence of spin-orbit (SO) interaction on various surface features. The interest in complex low-dimensional systems has grown enormously over the last years not only because of their technological relevance but even more because of the exciting new physics that may be explored in these fascinating designed compositions.[2,3] Prototype systems concerning surface features are found in the so-called Shockley surface states that, for example, develop at the (111) surfaces of almost all transition metals. A Shockley state is a solution of the Schrödinger equation with an energy lying in the gap of the bulk band structure and an imaginary momentum of the wave function perpendicular to the surface.[4,5] It is localized more or less in the topmost layer, it is partially decoupled from the bulk states, and follows a nearly free electron-like (NFE) behavior parallel to the surface with a parabolic dispersion crossing the Fermi level (E_F); thus it forms a quasi-two-dimensional electron gas (2DEG).[6] Considered as a quasiparticle model system, Shockley states have been employed for quantitative investigations of fundamental many-body properties of electron systems by inspecting the hole lifetime broadening, which reflects the different kinds of interactions (e.g., electron-electron, electron-phonon, and electron-defects interactions) in the solid.[7] The Shockley state can also cross the gap limit and appears merged into the bulk-states continuum. This is the situation when alkali atoms are adsorbed on the noble metal surfaces, where a strong electron scattering occurs and leads to a line-width broadening as well as a fading of the resulting spectroscopic feature.[8,9] Thereby, the state might be rather labeled as a Shockley-related surface resonance. On the other hand, the SO interaction is also probed by Shockley-state spectroscopy, as it is the case for Au(111).[10] As demonstrated by ARPES measurements given by Lashell *et al.*,[11] it is possible to observe two separate subbands along all in-plane directions corresponding to a Fermi surface that consists of two concentric cylinders with opposite spin directions.[10,12] The surface-induced removal of the inversion symmetry along the normal direction enhances the effects of the SO splitting, which actually diminishes when the inversion symmetry exists. Such an effect has not been commonly observed on the other surfaces of pure transition metals because the SO coupling is considered to be very weak, comparing to the one in Au(111), and cannot be detected by ARPES.[11,13] The study of the SO splitting as a function of controlled surface modifications has demonstrated that the splitting represents an important quantitative parameter for the investigation of interactions at surfaces and interfaces.[8] The contribution presented here investigates the modification of the *sp*-derived Shockley state of Pt(111) upon deposition of Ag overlayers and reflects the presence of a significant SO splitting. ARPES and scanning tunneling microscopy and spectroscopy (STM/STS) data are compared to one-step photoemission calculations based on first principles. A good agreement between experiment and theory is obtained and therefore the present study can contribute to the enhancement of our understanding of fundamental properties of the surface electronic structure.

II. EXPERIMENT

The STS experiments have been carried out with low-temperature microscope working under ultrahigh vacuum.

Spectroscopic curves, $dI/dV = f(V)$, were obtained using a lock-in amplifier and each curve is the average of many spectra recorded within a short acquisition time at identical points of the surface. The measurements have been recorded under open feedback loop (with the set point at -1.5 V, 1 nA) by adding a voltage modulation (of 20 mV, 760 Hz) using the lock-in technique. All ARPES spectra were collected at 50 K and the appropriate orientation (i.e., along high-symmetry directions) was fixed with the aid of LEED. The ARPES experiments have been performed at the X09LA-SIS beamline of the Swiss Light Source at Paul Scherrer Institute. The spectra have been recorded upon changing the photon energy and polarization of the light in order to obtain the best signal-to-background ratio of the surface features. The Ag layers were deposited on a clean Pt(111) substrate kept at room temperature as described elsewhere.[14]

III. THEORY

The electronic-structure as well as the photoemission calculations have been performed in a fully relativistic way for a true semi-infinite system using the upgraded version of the Munich SPR-KKR program package.[15] The theory of the relativistic one-step model of photoemission can be found, for example, in Ref. 16. Therefore, we restrict ourselves to presenting the so-called surface contribution only, which is of major importance for the quantitative calculation of surface-like intensity features.

Due to the surface contribution to the one-step model, special attention is paid to the long-range behavior of the surface barrier, which is included as an additional layer in the formalism. This layer is connected to the semi-infinite bulk region via the multiple-scattering theory. Hence, as has been known for a long time that the local-density approximation, and probably gradient-corrected schemes as well, are not able to provide a potential with the correct asymptotic behavior away from the crystal surface. Therefore, a density-functional-theory (DFT) surface potential gives only a good description for surface states that are located near the Fermi energy. This is not, however, a general shortcoming of DFT. It has been demonstrated, e.g., by Gunnarsson *et al.*,[17,18] that in the weighted-density approximation a model function describing the shape of the exchange-correlation hole can be tuned in such a way as to fulfill several physically important limiting conditions including the $1/z$ asymptotics of the potential outside a solid surface. *Ab initio* calculations incorporating the weighted-density approximation remain, however, relatively rare and have not yet been, to our knowledge, successfully applied to the study of surface-related electronic features. So far, an *ad hoc* adjustment of the potential barrier near the surface remains an arguably workable alternative. A realistic description of the surface potential is given through a spin-dependent Rundgren-Malmström barrier,[19] which connects the asymptotic regime $z < z_A$ to the bulk muffin-tin zero potential, $V_{\rm or}$, by a third-order polynomial in z spanning the range $z_A < z < z_E$. In other words, z_E defines the point where the surface region ends and the bulk region begins and z_I defines the position of the classical image plane.

In order to substantiate the theoretical discussion, we present the calculation scheme in detail in the following. Within the contribution $I^{\rm surf}(\epsilon_f,\mathbf{k}_\parallel)$ one takes care of the surface of the semi-infinite crystal:

$$I^{\rm surf}(\epsilon_f,\mathbf{k}_\parallel) = -\frac{1}{\pi}{\rm Im}\int {\rm d}\mathbf{r}\Psi_{\rm f}^{*\rm surf}(\mathbf{r})\triangle\Psi_{\rm i}^{\rm surf}(\mathbf{r}), \tag{1}$$

with

$$\Psi_i^{\rm surf}(\mathbf{r}) = \int d\mathbf{r}' G^+_{1\rm surf}(\mathbf{r},\mathbf{r}')\triangle^*\Psi_f^{\rm surf}(\mathbf{r}'). \tag{2}$$

In the case of a z-dependent barrier potential, $V_B = V_B(z)$, the initial- and final-state wave fields have to be calculated numerically in the surface region. Both wave fields, $\Psi_i^{\rm surf}(\mathbf{r})$ and $\Psi_f^{\rm surf}(\mathbf{r})$, can be decomposed into z-dependent and the corresponding parallel components,

$$\Psi_i^{\rm surf}(\mathbf{r}) = \sum_{\mathbf{g}} \phi_{1\mathbf{g}}(z)e^{i\mathbf{k}_{1\mathbf{g}\parallel}(\mathbf{r}-\mathbf{c}_1)_\parallel}, \tag{3}$$

$$\Psi_f^{\rm surf}(\mathbf{r}) = \sum_{\mathbf{g}} \psi_{2\mathbf{g}}(z)e^{i\mathbf{k}_{2\mathbf{g}_\parallel}(\mathbf{r}-\mathbf{c}_1)_\parallel}, \tag{4}$$

with the regular solutions of the Schrödinger equation, $\phi_{1\mathbf{g}}$ and $\psi_{2\mathbf{g}}$, to the reciprocal lattice vector, $\mathbf{g}$, for $V_B(z)$ in the range $-\infty < z < c_{1z}$. The value c_{1z} defines the point where the surface potential goes smoothly into the inner potential of the bulk crystal. It follows, first for the final state, as

$$\psi_{2\mathbf{g}}(z) = W^{2+}_{o\mathbf{g}}(z) + c^{2-}_{o\mathbf{g}}W^{2-}_{o\mathbf{g}}(z), \tag{5}$$

with the wave functions $W^{2+}_{o\mathbf{g}}$ and $W^{2-}_{o\mathbf{g}}$ traveling in $\pm z$ directions through the barrier. Far from the boundary between surface and bulk these two solutions of the Schrödinger equation can be written in terms of the well-known Whittaker functions. Starting with the asymptotic expansions for $W^{2-}_{o\mathbf{g}}$ and $W^{2+}_{o\mathbf{g}}$, which can be derived from the following expressions:

$$W^{2-}_{o\mathbf{g}}(z) = \frac{2e^{-ik_{1\mathbf{g}z}(z-z_1)} - 2ik_{1\mathbf{g}z}(z-z_1)^{\frac{i}{4k_{1\mathbf{g}z}}}}{\Gamma\left(1+\frac{i}{4k_{1\mathbf{g}z}}\right)} \times \left\{\sum_{n=0}^{S-1}\frac{\left(1-\frac{i}{4k_{1\mathbf{g}z}}\right)_{(n)}\left(-\frac{i}{4k_{1\mathbf{g}z}}\right)_{(n)}}{n!(-2ik_{1\mathbf{g}z})^n}\frac{1}{(z-z_1)^n}\right\} + O(|z|^{-S}), \tag{6}$$

and

$$W^{2+}_{o\mathbf{g}}(z) = \left[W^{2-}_{o\mathbf{g}}(z)\right]^*, \tag{7}$$

one can calculate the final state by numerical integration through the barrier potential, $V_B(z)$. The wave function, $\psi_{2\mathbf{g}}$, and its derivative must be continuous across the boundary between surface and bulk, which is defined by the so-called image plane, $z_{\rm im}$,

$$W^{2+}_{o\mathbf{g}}(z_{\rm im}) + c^{2-}_{o\mathbf{g}}W^{2-}_{o\mathbf{g}}(z_{\rm im}) = u^+_{o\mathbf{g}} + u^{-l}_{o\mathbf{g}}, \tag{8}$$

$$W^{2+'}_{o\mathbf{g}}(z_{\rm im}) + c^{2-}_{o\mathbf{g}}W^{2-'}_{o\mathbf{g}}(z_{\rm im}) = ik^+_{2\mathbf{g}}(u^+_{o\mathbf{g}} - u^{-l}_{o\mathbf{g}}). \tag{9}$$

The coefficients $u^+_{o\mathbf{g}}$ and $u^{-l}_{o\mathbf{g}}$, representing the bulk solution at the image plane, are connected by the following equation:

$$u^{-l}_{o\mathbf{g}} = R^{-+}_{\mathbf{g}\mathbf{g}'}u^+_{o\mathbf{g}'} + \{R^{--}P^-B(1 - P^+R^{+-}P^-B)^{-1}P^+R^{++}\}_{\mathbf{g}\mathbf{g}'}u^+_{o\mathbf{g}'}. \tag{10}$$

Herein $R^{\pm\pm}$ and $P^{\pm}$ denote the reflection and transmission coefficients and the propagators of the barrier. B denotes the bulk reflection matrix. From the above linear system of equations the unknown coefficients $u^{+}_{o\mathbf{g}}$ and $c^{2-}_{o\mathbf{g}}$ can be calculated. At this stage the final-state amplitude $u^{+}_{1\mathbf{g}}$ at the first bulk layer can be easily obtained by standard KKR multiple-scattering techniques:

$$u^{+}_{1\mathbf{g}} = \{(1 - P^{+}R^{-+}P^{-})^{-1}P^{+}R^{++}\}_{\mathbf{g}\mathbf{g}'}u^{+}_{o\mathbf{g}'}. \tag{11}$$

With Eq. (12) the initial-state calculation starts by defining the wave function, $\phi_{1\mathbf{g}}$, in the region between the semi-infinite bulk and the surface barrier. Calculation of the initial state in the surface region gives

$$\phi_{1\mathbf{g}}(z) = a^{1+}_{o\mathbf{g}}(z) + c^{1-}_{o\mathbf{g}}W^{1-}_{o\mathbf{g}}(z), \tag{12}$$

with

$$a^{1+}_{\mathbf{g}}(z') = \frac{A_z e^{-i\mathbf{q}\cdot\mathbf{c}_1}}{2\omega c k^{+}_{1\mathbf{g}z'}}\int_{-\infty}^{z'} dz e^{-i(q_z + k^{+}_{1\mathbf{g}z})(z - c_{1z})}V'_B\psi^{*}_{2\mathbf{g}}(z). \tag{13}$$

The corresponding plane-wave amplitude, $a^{+}_{1\mathbf{g}}$, appears directly proportional to the gradient of the surface potential. The amplitude, $d^{+}_{1\mathbf{g}}$, corrected for all multiple scattering between the semi-infinite bulk and the surface potential, is shown in Eq. (18). This quantity enters directly the surface contribution of the photocurrent. Because of the multiple scattering between bulk and surface defined by Eqs. (16) and (17), the spin-orbit interaction present in the gradients of the single-ion-core potentials is accumulated in $d^{+}_{1\mathbf{g}}$, which, on the other hand, represents the surface-state wave function.

The wave field, $a^{+}_{1\mathbf{g}}$, represents the initial state emitted by the barrier. Again, after numerical integration through the surface potential, the initial-state wave field and its derivative have to be matched to the bulk solution at the boundary, z_{im},

$$a^{1+}_{o\mathbf{g}}(z_{\mathrm{im}}) + c^{1-}_{o\mathbf{g}}W^{1-}_{o\mathbf{g}}(z_{\mathrm{im}}) = (1 + M)_{\mathbf{g}\mathbf{g}'}d^{+}_{o\mathbf{g}'} + N_{\mathbf{g}\mathbf{g}'}b^{-}_{o\mathbf{g}'}, \tag{14}$$

$$a^{1+'}_{o\mathbf{g}}(z_{\mathrm{im}}) + c^{1-}_{o\mathbf{g}}W^{1-'}_{o\mathbf{g}}(z_{\mathrm{im}}) = ik^{+}_{1\mathbf{g}}(1 - M)_{\mathbf{g}\mathbf{g}'}d^{+}_{o\mathbf{g}'} - ik^{+}_{1\mathbf{g}}N_{\mathbf{g}\mathbf{g}'}b^{-}_{o\mathbf{g}'}. \tag{15}$$

From this linear system of equations the unknown coefficients, $d^{+}_{o\mathbf{g}}$ and $c^{1-}_{o\mathbf{g}}$, can be calculated. The amplitude, $b^{-}_{o\mathbf{g}}$, defines the initial state that is emitted by the bulk crystal. For the matrices M and N it follows:

$$M_{\mathbf{g}\mathbf{g}'} = R^{-+}_{\mathbf{g}\mathbf{g}'} + \{R^{--}P^{-}B(1 - P^{+}R^{+-}P^{-}B)^{-1}P^{+}R^{++}\}_{\mathbf{g}\mathbf{g}'}, \tag{16}$$

$$N_{\mathbf{g}\mathbf{g}'} = \{R^{--}(1 - P^{-}BP^{+}R^{+-})^{-1}P^{-}\}_{\mathbf{g}\mathbf{g}'}. \tag{17}$$

Again, $R^{\pm\pm}$ and $P^{\pm}$ denote the reflection and transmission coefficients and the propagators of the barrier. B denotes the bulk reflection matrix but now for the initial state. With the multiple-scattering equations shown above the coupling of the barrier potential to the semi-infinite bulk is described explicitly. The amount of spin-orbit splitting observable in a corresponding surface-state resonance is therefore controlled by the strength of the reflection properties of the semi-infinite bulk, which is coupled to the surface potential via multiple scattering. Moreover, the photoemission takes care of matrix-element effects in calculating the final- and initial-state wave fields again by using multiple scattering theory. The coefficients that define the final- and initial-state wave fields have been calculated using the bulk reflection and surface-barrier scattering matrices. In this way, the coefficients are responsible for all symmetry considerations of a Rashba-split surface-state resonance that are discussed in the literature.

This is demonstrated by the following equation, which defines the initial-state amplitude, $d^{+}_{1\mathbf{g}}$, at the first bulk layer corrected for all multiple-scattering events:

$$d^{+}_{1\mathbf{g}} = \{(1 - P^{+}R^{+-}P^{-}B)^{-1}P^{+}R^{++}\}_{\mathbf{g}\mathbf{g}'}d^{+}_{o\mathbf{g}'} + \{(1 - P^{+}R^{+-}P^{-}B)^{-1}P^{+}R^{+-}P^{-}\}_{\mathbf{g}\mathbf{g}'}b^{-}_{1\mathbf{g}'}. \tag{18}$$

The final evaluation of the surface contribution gives

$$I^{\mathrm{surf}}(\mathbf{k}_{\parallel},\epsilon_f) = -\frac{1}{\pi}\frac{A_z}{2\omega c}\mathrm{Im}\left\{e^{i\mathbf{q}_{\parallel}\cdot\mathbf{c}_{1\parallel}}\sum_{\mathbf{g}}\int_{-\infty}^{c_{1z}} dz\psi_{2\mathbf{g}}(z)V'_B\phi_{1\mathbf{g}}(z)e^{iq_z z}\right\}, \tag{19}$$

where A_z is the z component of the amplitude, $\mathbf{A}_0$ and $\mathbf{q}$ is the wave vector of the photon field.

Due to the theoretical approach described above, the concrete mechanism that mediates the spin-orbit interaction is no longer hidden as in a pure slab or semi-infinite half-space electronic structure calculation. In fact, one is able to describe the Rashba splitting of a surface feature via multiple-scattering formulas and, in consequence, one can tune the magnitude of the Rashba splitting in more detail.

IV. RESULTS AND DISCUSSION

The Shockley state of Pt(111) has been the subject of debate during the last decade. While early ARPES studies have suggested its presence in the occupied region of the band structure at a binding energy of about 400 meV below E_F,[20] recent STS measurements together with electronic structure calculations have shown that it is situated above E_F and exhibits a band splitting due to the Rashba-Bychkov (RB) spin-orbit coupling.[21] By taking advantage of our ability to tune the photon energy and light polarization of the synchrotron radiation, we have seen through careful ARPES investigations that no Shockley state/resonance band is occurring around the $\bar{\Gamma}$ point of the surface Brillouin zone (SBZ). Moreover, our *ab initio* band-structure calculations, shown in Fig. 1, agree with this finding and provide an SO-split band entirely located above E_F in the inverted sp-like band gap. Its energetic dispersion can be described within the RB model as

$$E_{\pm}(\vec{k}) = E_0 + \frac{\hbar^2 k^2}{2m^{\star}} \pm \alpha_R|k|, \tag{20}$$

where $\pm$ refers to the two opposite spin states. The crossing of the two bands lies at the $\bar{\Gamma}$ point at a binding energy of about -355 meV (see Ref. 22) and it is in a good agreement with Ref. 21. Strong polarization dependence due to the linearly polarized light is observed in the spin up-down spectra. The Shockley state shows more straight-like dispersion due

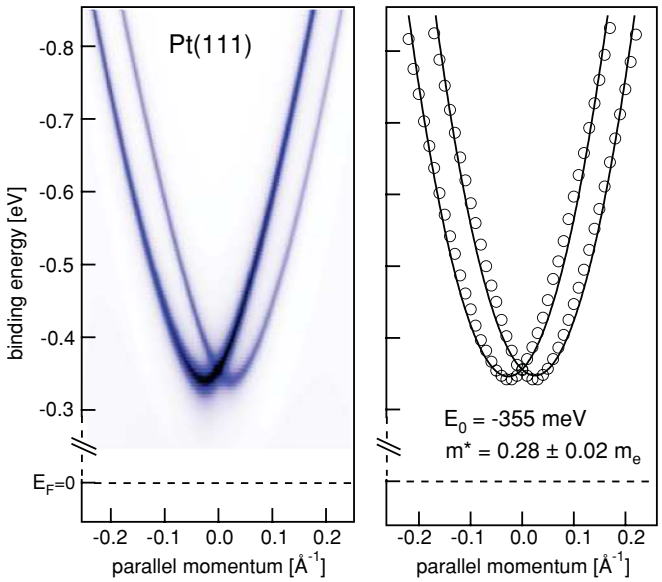

FIG. 1. (Color online) Dispersion of the Pt(111) Shockley surface state obtained by electronic-structure calculations. Left panel: Color-scale intensity map; right panel: dispersion of the momentum distribution curve maxima (circles) approximated by a parabolic fit using Eq. (20) (solid line).

to the coupling with the nearby bulk states; therefore, we observe a slight deviation from the NFE parabolic behavior (right panel of Fig. 1) giving a reduced effective mass $m^\star = \hbar^2[d^2E(k)/dk^2]^{-1} = 0.28 \pm 0.02\ m_e$, where m_e is the bare electron mass. The amplitude of the spin splitting, k_0, is proportional to the Rashba parameter, $\alpha_R = \hbar^2 k_0/m^\star$, and it is estimated here to be 0.026 ± 0.003 Å^{-1}, which appears larger than the one measured on Au(111) and represents therefore the highest value so far obtained for Shockley states *at* metal surfaces. The large Pt(111) splitting is partially ascribed to the high atomic number, Z, of Pt.

Actually, similar splittings have been studied in many other systems, namely, in bare semimetal surfaces,[23–25] in heavy-metal-induced surface alloys formed on noble metals[26–30] or on semiconductor[31–34] surfaces, and in single metal monolayer[35] or in atomic quantum wires[36] deposited respectively on semiconductor surfaces. Also, numerous investigations have been devoted to its modification upon deposition of metallic layers,[37–40] adsorption of different gases,[41–44] or even evaporation of well-ordered layers of organic molecules on the surface.[45] It has often been discussed that two parameters influence the size of the band splitting: the atomic SO interaction and the gradients of the surface potential directed perpendicular and parallel to the surface. For example, in an ordered alloy like Bi/Ag(111) the relaxation of the surface atoms induces a gradient of the surface potential providing a SO splitting so large that it is possible to estimate its magnitude by STS measurements of the local density of states (LDOS) showing a van-Hove-like singularity.[46] Also, the atomic SO interaction of the surface atoms should be taken into consideration, e.g., in order to explain the significant difference in the size of SO splitting between Bi/Ag(111)[46] and Sb/Ag(111).[27]

In the following, we present the first STS and ARPES data measured in the Ag/Pt(111) system and limit ourselves to the behavior of the surface state that occurs within the bulk-states continuum upon deposition of Ag and can, henceforth, be described as a surface resonance. Note that this system shows interesting structural properties;[14,47,48] previous and our STM investigations have shown that Ag grows layer by layer on Pt(111) at 300 K up to a coverage of 6–9 monolayers (ML) with an (111) orientation.[49] As shown in Fig. 2, at a closed monolayer the Ag atoms are coherently strained and form a compressed pseudomorphic layer appearing flat in the STM image. In contrast, the second monolayer displays ordered metastable superstructure patterns consisting of alternating domains with fcc and hcp stacking separated by partial misfit dislocation lines seen as dark stripes in the STM images.[49] The third monolayer (in Fig. 2) exhibits certain structural ordering of hexagonally arranged areas surrounded by partial dislocation walls. Note that the sample has been kept at $T \leqslant 300$ K during preparation and measurements and, in this case, the formation of alloy is unlikely.

The three curves in the right part of Fig. 2 correspond to low-temperature STS measurements (80 K) on 2-, 3-, and 4-ML-thick films of Ag on Pt(111). These spectroscopic data give the differential conductance profile, dI/dV, which here is proportional mainly to the local density of the surface resonance and with the maximum of the measured feature corresponding to the bottom of the band. A significant change of the surface-resonance parameters depending on the Ag thickness is observed. Compared to its position on clean Pt(111), i.e., $E_0 = -355$ meV, the surface resonance shifts downward on the covered surface by 2 ML of Ag and

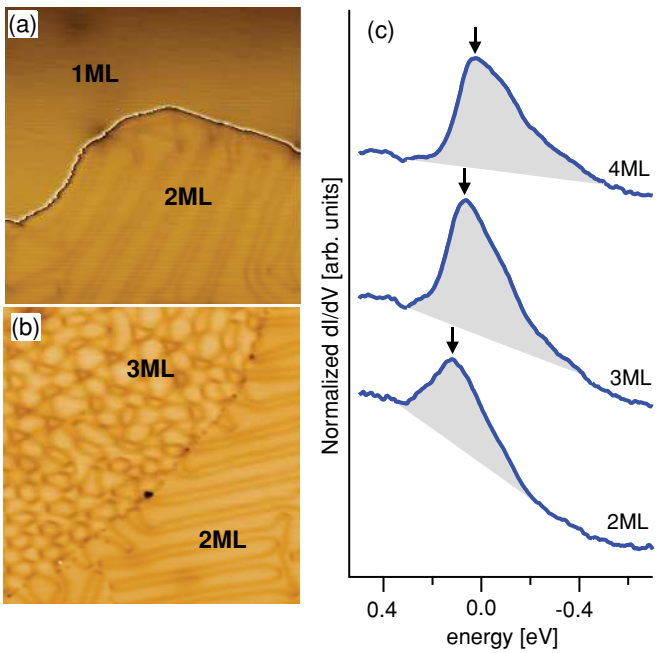

FIG. 2. (Color online) Room-temperature STM images (60×60 nm^2) of (a) 1.5 ML and (b) 2.5 ML Ag thin films deposited on Pt(111). (c) Differential conductivity curves measured by STS in the different Ag-covered surface regions. The curve maxima give the energy position of the surface resonance.

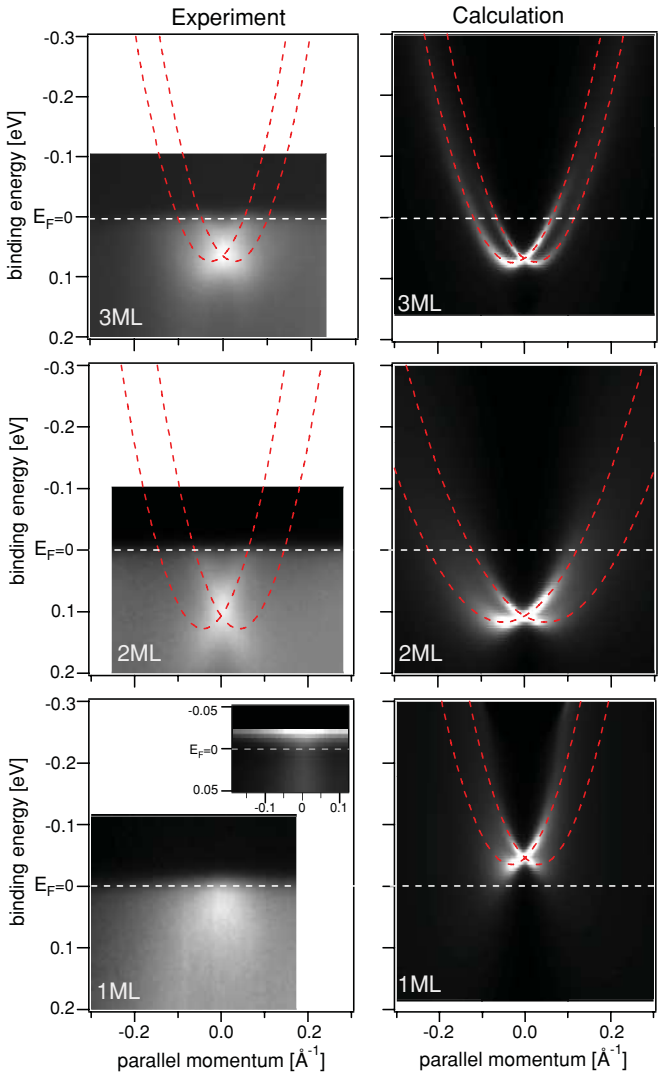

FIG. 3. (Color online) Surface-resonance bands obtained by ARPES measurements (left panels) and by first-principles calculations (right panels) on Pt(111) surfaces covered by 1, 2, and 3 monolayers, respectively. The ARPES data have been recorded at normal emission along the $\bar{\Gamma}$-$\bar{K}$ direction and at $T = 50$ K. For 1 ML, the inset shows the ARPES intensity map divided by the Fermi function. The band dispersions are approximated by parabolic curves (dashed red lines).

becomes partially occupied with a maximum binding energy of about $E_0 = 114 \pm 5$ meV. At a higher thickness, the bottom of the band shifts upward to $E_0 = 65 \pm 5$ meV at 3 ML and to $E_0 = 40 \pm 5$ meV at 4 ML and continuously converges to the position of the surface state on bare Ag(111). This energy shift is also demonstrated by ARPES and calculations, which, furthermore, give the effective mass and the SO band splitting.

Figure 3 displays ARPES intensity maps and the corresponding total spectral-density maps of the surface-resonance band obtained for different thicknesses of Ag on Pt(111). The characteristic parameters of the band dispersion, inferred from a fit using Eq. (20), are given in Table I. At 1 ML, the ARPES intensity map, corrected by the Fermi function, as well as the theory suggest a downward shift of the dispersive band with a maximum binding energy still in the regime of empty states, $E_0^{\mathrm{cal}} = -46$ meV. The lowest energy is obtained at 2 ML ($E_0^{\mathrm{cal}} = 109$ meV, $E_0^{\mathrm{exp}} = 107 \pm 5$ meV), then the surface resonance moves back upward ($E_0^{\mathrm{cal}} = 67$ meV, $E_0^{\mathrm{exp}} = 65 \pm 5$ meV) at 3 ML. The energy shift observed in Ag/Pt(111) is apparently different from those obtained in other systems like Ag/Cu(111)[51,52] and Ag/Au(111),[38,53] where the energy displacement is monotonously changing and, usually, toward a unique direction. Likewise, the value of the effective mass is closely connected to the film thickness (see Table I), suggesting a large Ag-induced modification of the in-plane gradient of the surface potential. We distinguish a difference in the band curvature between the calculated and experimental results, in particular for 2 ML, which can be attributed to the surface reconstruction inducing a change of the in-plane surface potential. This effect is not observed at the Au(111) surface[10] characterized by the well-known herringbone reconstruction.[54] We believe that the superpotential of the reconstruction is rather weak in the case of Au(111) compared to Ag/Pt(111). Surprisingly, the SO splitting is strongly enlarged through Ag deposition. Close inspection of the ARPES data—shown in Fig. 3—yields to an estimation of a maximum SO, obtained at 2 ML, of about 0.051 ± 0.007 Å^{-1}, which is larger than those observed at both the Ag(111) and Pt(111) surfaces. As Table I indicates, the magnitude of the Rashba splitting is reduced when the thickness of the Ag layer exceeds 2 ML.

By keeping in mind that the actual surface presents no alloy, the hypothesis of a strong in-plane surface potential inducing high SO splitting is not satisfied, instead, the mechanism behind it is found in the multiple scattering between bulk and surface. Indeed, the SO interaction determined from a single ion-core potential contains no information about the parallel momentum ($k_{||}$) but the surface potential is well ordered according to the two-dimensional crystal structure of a given system. The multiple scattering then transforms the SO information into a $k_{||}$ splitting of a surface resonance. This scattering procedure is realized by the bulk reflection matrix B, a quantity which is developed into the two-dimensional reciprocal lattice vectors of the corresponding surface. B contains the complete electronic structure information of the semi-infinite bulk of the system. From our formalism, i.e., Eqs. (16) and (17), it follows that the scattering is, to the first order, proportional to B and, in consequence, the amount of SO splitting of the surface resonance directly scales with $|B|$. In detail, when reducing the off-diagonal elements of B, e.g., when reducing the influence of the two-dimensional reciprocal lattice, the transfer of $k_{||}$-splitting decreases and so does the Rashba splitting. This mechanism can be considered as the driving parameter of increased SO splitting beyond a virtual and straightforward approach interpolating between adsorbate and adsorbent properties.[38]

On the other hand, we observe in both the ARPES data and the calculation results of Fig. 3 a peculiar variation of the electron intensity as a function of $k_{||}$. In particular, on the sides of the bands away from the SBZ center, the intensity is significantly reduced and spread-out into the bulk continuum. This behavior, which has never been observed so markedly on other surfaces, reflects the presence of a strong

TABLE I. Characteristic quantities inferred from the Shockley state and the surface-resonance dispersions on bare and Ag-covered Pt(111) surfaces, respectively. The columns are the bottom of the band, E_0, effective mass, $m^\star$, wave-vector offset, k_0, and Rashba parameter, α_R. Values derived from ARPES, STS, and calculation are given. For comparison, the second part of the table shows the surface-state parameters obtained for other systems that are characterized by high spin-orbit splittings.

Material	$E_0(meV)$	$m^\star$ (m_e)	k_0 (Å^{-1})	α_R (eV Å)
Pt(111)$^{\text{calculation}}$	-355	0.28 ± 0.02	0.026 ± 0.003	0.67 ± 0.03
1ML Ag/Pt(111)$^{\text{calculation}}$	-46	0.38 ± 0.05	0.033 ± 0.007	0.66 ± 0.06
2ML Ag/Pt(111)$^{\text{ARPES}}$	107 ± 5	0.32 ± 0.1	0.043 ± 0.017	1.02 ± 0.1
2ML Ag/Pt(111)$^{\text{STS}}$	114 ± 5			
2ML Ag/Pt(111)$^{\text{calculation}}$	109	0.95 ± 0.04	0.051 ± 0.007	0.41 ± 0.04
3ML Ag/Pt(111)$^{\text{ARPES}}$	65 ± 5	0.29 ± 0.1	0.027 ± 0.013	0.71 ± 0.1
3ML Ag/Pt(111)$^{\text{STS}}$	65 ± 5			
3ML Ag/Pt(111)$^{\text{calculation}}$	67	0.42 ± 0.02	0.028 ± 0.003	0.51 ± 0.03
Au(111)[a]	487 ± 1	0.255	0.013	0.33
Bi/Ag(111)[b]	335	-0.35	0.13	3.05
Bi/Si(111)[c]	1200	0.7	0.126	1.37
Pb/Ge(111)[d]		0.028	0.028 ± 0.002	0.24 ± 0.02

[a]References 11 and 50.
[b]Reference 26.
[c]Reference 33.
[d]Reference 35.

coupling process between the surface resonance and the nearby Pt bulk states. In fact, the absence of supporting gap in the projected band structure below E_F favors this process through inelastic electron-electron scattering. In addition, as predicted by theory,[55] when $k_{||}$ increases the surface resonance acquires a bulk-like character with a larger penetration into the bulk, thereby, it overlaps with the continuum and becomes indistinct. This interpretation is supported by the observation of a peak-like structure in the dI/dV profiles of Fig. 2, instead of a constant LDOS. From the calculation that corroborates the ARPES data, we observe that the surface resonance at higher thicknesses exhibits a narrow line width, which reflects a decrease of the electron scattering with the bulk states due to a building of Ag band gap around the $\bar{\Gamma}$ point. The surface resonance regains more and more Shockley-state character as soon as the Ag film becomes thicker.

V. CONCLUSIONS

Here, we reported the modification of the Pt(111) Shockley state caused by deposition of Ag monolayers. The corresponding state is rather described as a surface resonance since it appears directly coupled with the bulk states. We have shown that both techniques ARPES and STS are in good agreement with the spectroscopical calculations, in particular, for the energy position of the surface resonance versus the Ag thickness. We have shown the existence of a sizable SO splitting, one of the highest so far observed, in the surface-resonance state band. This effect is thought to be closely dependent on the multiple scattering between bulk and surface.

ACKNOWLEDGMENTS

We gratefully thank P. Varga, M. Schmid, and A. Buchsbaum (from Vienna, Austria) for the access to their instrument and for the STM images and also the beamline staff of X09LA at the Swiss Light Source for their excellent technical support. Financial support by the Deutsche Forschungsgemeinschaft and the Bundesministerium für Bildung und Forschung is gratefully acknowledged.

*azzedine.bendounan@synchrotron-soleil.fr
†juergen.braun@cup.uni-muenchen.de

[1]F. Manghi, V. Bellini, J. Osterwalder, T. J. Kreutz, P. Aebi, and C. Arcangeli, Phys. Rev. B **59**, R10409 (1999).
[2]P. A. Loukakos, M. Lisowski, G. Bihlmayer, S. Blügel, M. Wolf, and U. Bovensiepen, Phys. Rev. Lett. **98**, 097401 (2007).
[3]D. Hsieh *et al.*, Science **323**, 919 (2008).
[4]I. E. Tamm, Phys. Z. Sowjetunion **1**, 733 (1932).
[5]W. Shockley, Phys. Rev. **56**, 317 (1939).
[6]S. G. Davison and Stęślicka, in *Basic Theory of Surface States* (Oxford University Press, Oxford, New York, 1992).
[7]P. M. Echenique, R. Berndt, E. V. Chulkov, T. Fauster, A. Goldmann, and U. Höfer, Surf. Sci. Rep. **52**, 219 (2004).
[8]F. Forster, A. Bendounan, J. Ziroff, and F. Reinert, Surf. Sci. **600**, 3870 (2006).
[9]J. M. Carlsson and B. Hellsing, Phys. Rev. B **61**, 13973 (2000).

[10]G. Nicolay, F. Reinert, S. Hüfner, and P. Blaha, Phys. Rev. B **65**, 033407 (2001).
[11]S. LaShell, B. A. McDougall, and E. Jensen, Phys. Rev. Lett. **77**, 3419 (1996).
[12]M. Hoesch, V. Muntwiler, V. N. Petrov, M. Hengsberger, L. Patthey, M. Shi, M. Falub, T. Greber, and J. Osterwalder, Phys. Rev. B **69**, 241401 (2004).
[13]F. Reinert, J. Phys. Condens. Matter **15**, S693 (2003).
[14]K. Aït-Mansour, A. Buchsbaum, P. Ruffieux, M. Schmid, P. Gröning, P. Varga, R. Fasel, and O. Gröning, Nano Lett. **8**, 2035 (2008).
[15]H. Ebert *et al.*, in *The Munich*SPR-KKR *Package*, version 5.4, [http://olymp.cup.uni-muenchen.de/ak/ebert/SPRKKR].
[16]J. Braun and M. Donath, J. Phys. Condens. Matter **16**, 2539 (2004).
[17]O. Gunnarsson, M. Jonson, and B. I. Lundqvist, Phys. Rev. B **20**, 3136 (1979).
[18]R. O. Jones and O. Gunnarsson, Rev. Mod. Phys. **61**, 689 (1989).
[19]G. Malmström and J. Rundgren, Comput. Phys. Commun. **19**, 263 (1980).
[20]N. Memmel and E. Bertel, Phys. Rev. Lett. **75**, 485 (1995).
[21]J. Wiebe, F. Meier, K. Hashimoto, G. Bihlmayer, S. Blügel, P. Ferriani, S. Heinze, and R. Wiesendanger, Phys. Rev. B **72**, 193406 (2005).
[22]Energies above E_F are indicated by the negative sign and those below E_F by positive.
[23]Y. M. Koroteev, G. Bihlmayer, J. E. Gayone, E. V. Chulkov, S. Blügel, P. M. Echenique, and P. Hofmann, Phys. Rev. Lett. **93**, 46403 (2004).
[24]K. Sugawara, T. Sato, S. Souma, T. Takahashi, M. Arai, and T. Sasaki, Phys. Rev. Lett. **96**, 46411 (2006).
[25]T. Hirahara, T. Nagao, I. Matsuda, G. Bihlmayer, E. V. Chulkov, Y. M. Koroteev, P. M. Echenique, M. Saito, and S. Hasegawa, Phys. Rev. Lett. **97**, 146803 (2006).
[26]C. R. Ast, J. Henk, A. Ernst, L. Moreschini, M. C. Falub, D. Pacilé, P. Bruno, K. Kern, and M. Grioni, Phys. Rev. Lett. **98**, 186807 (2007).
[27]L. Moreschini *et al.*, Phys. Rev. B **79**, 075424 (2009).
[28]L. Moreschini, A. Bendounan, H. Bentmann, M. Assig, K. Kern, F. Reinert, J. Henk, C. R. Ast, and M. Grioni, Phys. Rev. B **80**, 035438 (2009).
[29]C. R. Ast *et al.*, Phys. Rev. B **77**, 081407 (2008).
[30]I. Gierz, J. Stadtmüller, J. Vuorinen, M. Lindroos, F. Meier, J. H. Dil, K. Kern, and C. R. Ast, Phys. Rev. B **81**, 245430 (2010).
[31]J. Nitta, T. Akazaki, H. Takayanagi, and T. Enoki, Phys. Rev. Lett. **78**, 1335 (1997).
[32]B. Das, S. Datta, and R. Reifenberger, Phys. Rev. B **41**, 8278 (1990).
[33]I. Gierz, T. Suzuki, E. Frantzeskakis, S. Pons, S. Ostanin, A. Ernst, J. Henk, M. Grioni, K. Kern, and C. R. Ast, Phys. Rev. Lett. **103**, 046803 (2009).
[34]E. Frantzeskakis, S. Pons, and M. Grioni, Phys. Rev. B **82**, 085440 (2010).
[35]K. Yaji, Y. Ohtsubo, S. Hatta, H. Okuyama, K. Miyamoto, T. Okuda, A. Kimura, H. Namatame, M. Taniguch, and T. Aruga, Nature Commun. **1**, 9307 (2010).
[36]I. Barke, F. Zheng, T. K. Rügheimer, and F. J. Himpsel, Phys. Rev. Lett. **97**, 226405 (2006).
[37]E. Rotenberg, J. W. Chung, and S. D. Kevan, Phys. Rev. Lett. **82**, 4066 (1999).
[38]D. Malterre, B. Kierren, Y. Fagot-Revurat, S. Pons, A. Tejeda, C. Didiot, H. Cercellier, and A. Bendounan, New J. Phys. **9**, 391 (2007).
[39]A. M. Shikin, A. Varykhalov, G. V. Prudnikova, D. Usachov, V. K. Adamchuk, Y. Yamada, Y. D. Riley, and O. Rader, Phys. Rev. Lett. **100**, 057601 (2008).
[40]A. G. Rybkin, A. M. Shikin, V. K. Adamchuk, D. Marchenko, C. Biswas, A. Varykholov, and O. Rader, Phys. Rev. B **82**, 233403 (2010).
[41]M. Hochstrasser, J. G. Tobin, E. Rotenberg, and S. D. Kevan, Phys. Rev. Lett. **89**, 216802 (2002).
[42]F. Forster, S. Hüfner, and F. Reinert, J. Phys. Chem. B **108**, 14692 (2004).
[43]F. Forster, A. Bendounan, F. Reinert, V. G. Grigoryan, and M. Springborg, Surf. Sci. **601**, 5595 (2007).
[44]L. Moreschini, A. Bendounan, C. R. Ast, F. Reinert, M. Falub, and M. Grioni, Phys. Rev. B **77**, 115407 (2008).
[45]J. Ziroff, P. Gold, A. Bendounan, F. Forster, and F. Reinert, Surf. Sci. **603**, 354 (2009).
[46]C. R. Ast, G. Wittich, P. Wahl, R. Vogelgesang, D. Pacilé, M. C. Falub, L. Moreschini, M. Papagno, M. Grioni, and K. Kern, Phys. Rev. B **75**, 201401 (2007).
[47]H. Brune, M. Giovannini, K. Bromann, and K. Kern, Nature (London) **394**, 451 (1998).
[48]P. Ruffieux, K. Aït-Mansour, A. Bendounan, R. Fasel, L. Patthey, P. Gröning, and O. Gröning, Phys. Rev. Lett. **102**, 86807 (2009).
[49]H. Röder, K. Bromann, H. Brune, and K. Kern, Surf. Sci. **376**, 13 (1997).
[50]F. Reinert, G. Nicolay, S. Schmidt, D. Ehm, and S. Hüfner, Phys. Rev. B **63**, 115415 (2001).
[51]A. Bendounan, H. Cercellier, Y. Fagot-Revurat, B. Kierren, V. Yu Yurov, and D. Malterre, Phys. Rev. B **67**, 165412 (2003).
[52]A. Bendounan, F. Forster, J. Ziroff, F. Schmitt, and F. Reinert, Phys. Rev. B **72**, 075407 (2005).
[53]H. Cercellier, C. Didiot, Y. Fagot-Revurat, B. Kierren, L. Moreau, D. Malterre, and F. Reinert, Phys. Rev. B **73**, 195413 (2006).
[54]J. V. Barth, H. Brune, G. Ertl, and R. J. Behm, Phys. Rev. B **42**, 9307 (1990).
[55]P. M. Echenique, J. Osma, M. Machado, V. M. Sikin, E. V. Chulkov, and J. M. Pitarke, Prog. Surf. Sci. **67**, 271 (2001).